Available online at www.sciencedirect.com
SCIENCE DIRECT®
International Journal of Heat and Mass Transfer 48 (2005) 3411–3422
International Journal of HEAT and MASS TRANSFER
www.elsevier.com/locate/ijhmt

Investigation of mixing mechanisms and energy balance in reactive extrusion using three-dimensional numerical simulation method

Linjie Zhu [a,1], Kwabena A. Narh [a,*], Kun S. Hyun [b,2]

[a] Department of Mechanical Engineering, New Jersey Institute of Technology, Newark, NJ 07102-1982, USA
[b] Polymer Processing Institute and Otto H. York Department of Chemical Engineering, New Jersey Institute of Technology, Newark, NJ 07102-1982, USA

Received 18 March 2004; received in revised form 11 November 2004

Abstract

The polymerization of ε-caprolactone in fully-filled conveying elements of co-rotating twin-screw extruders was analyzed with three-dimensional numerical simulation method. The effects of screw rotational speed, geometry of screw element, and initial conversion at the channel inlet on polymerization progression were studied. The simulation results show that polymerization is accelerated with increasing screw pitch, due to the increase in mixing intensity. With increasing screw rotational speed, the reaction could either slow down or speed up, depending on the viscosity of the reaction system. It is found that the advancement of polymerization depends on the competition among heat from reaction, viscous dissipation and heat loss through the wall surfaces.

Keywords: Numerical simulation; Polymerization; Energy; Extrusion; Mixing

1. Introduction

In a reactive extrusion process, the synthesis or modification of a polymeric material takes place simultaneously with the processing and shaping of the final product. This is an efficient method for continuous polymerization of monomers and chemical modification of existing polymers, and is viewed as a complex reaction engineering process that combines the traditionally separated operations, i.e., polymer chemistry (polymerization or chemical modification) and extrusion (blending, compounding, structuring, devolatilization, and eventually shaping), into a single process in a screw extruder [1–3]. Chemical reactions, such as bulk polymerization, graft reaction, inter-chain co-polymer formation, coupling/crosslinking reactions, controlled degradation, functionalization, and reactive blending, have been performed successfully with reactive extrusion [1–4].

The co-rotating twin screw extruders have been found very attractive for many reactive processing applications because of several inherent features, such as

* Corresponding author. Tel.: +1 973 596 3353; fax: +1 973 642 4282.
E-mail addresses: lxz4991@njit.edu (L. Zhu), narh@njit.edu (K.A. Narh), kshyun@polymers-ppi.org (K.S. Hyun).
[1] Present address: Polymer Processing Institute, New Jersey Institute of Technology, Newark, NJ 07102-1982, USA. Tel.: +1 973 596 5667; fax: +1 973 642 4282.
[2] Tel.: +1 973 596 3267; fax: +1 973 642 4594.

0017-9310/$ - see front matter © 2005 Elsevier Ltd. All rights reserved.
doi:10.1016/j.ijheatmasstransfer.2004.12.049

Nomenclature

A	area (m^2)
$A(i)$	area of element i (m^2)
a	coefficient related to the distribution of molecular weight in Eq. (7)
a_ϕ	parameter for free volume correction
C	conversion
C_p	specific heat (J/kg K)
E_a	activation energy for reaction (kJ/mol)
E_b	activation energy for flow of bulk system (kJ/mol)
E_s	activation energy for flow of solution system (kJ/mol)
ΔH	reaction heat (kJ/kg)
h	heat transfer coefficients at barrel surface (W/m^2 K)
K	kinetics constant
k	thermal conductivity (W/m K)
$[I]$	initial initiator concentration
$[M]$	monomer concentration
M	molecular weight
N	screw rotating speed (rpm)
N_e	number of elements
n	pseudoplastic index
P	pressure (Pa)
Q_R	rate of reaction heat generation (kJ/m^3 s)
Q	flow rate (m^3/s)
T	temperature (K)
t	reaction time (s)
U, V, W	velocity (m/s)

Greek symbols

α	the partial order related to the initiator
χ	drag flow coefficient
γ	shear rate (1/s)
λ	pressure flow coefficient
τ	shear stress (Pa)
ξ	parameter related to the reactive process in Eq. (15)
η	viscosity (Pa s)
ρ	density (kg/m^3)

Subscripts

0	initial or zero
D	drag flow
P	pressure flow

staging of sequential unit operations, removal of unreacted monomers and by-product, modular screw and barrel design, self-wiping structure, and excellent dispersive and distributive mixing [5]. However, the unique advantages of the twin-screw extruders also make the operations of the machine complicated. The twin-screw extruder is a device having multi-operational parameters, such as screw configuration, screw rotational speed, temperature, feeding rate and feeding protocol. It is not easy to couple these parameters, in order to carry out an optimum processing, especially for the complex reactive extrusion process. Consequently, numerical simulation has been used as an important method in optimizing extrusion processing [6].

One important characteristic of reactive extrusion is the non-isothermal progression of the reactive system in the extruder, which is associated with the energy sources in the system. There are three energy sources in a reactive system, including viscous dissipation, heat from reaction, and heat transfer through the barrel and screw surfaces. These energy sources compete with each other in reactive extrusion, affecting the advancement of reaction.

In the present study, the competition of energy sources in reactive extrusion was investigated with three-dimensional numerical simulation method, using a commercial Computational Fluid Dynamics (CFD) package, FLUENT 6.0. Polymerization of ε-caprolactone was used as a model system. The effects of screw rotational speed, geometry of screw elements, and initial conversion of the reaction system at the channel inlet on polymerization progression are discussed.

2. Simulation model

2.1. Model system

According to experimental studies by Gimenez et al. [7] and Poulesquen et al. [8], the bulk polymerization of ε-caprolactone follows a first order reaction equation:

$$\frac{d[M]}{dt} = -K[M] \tag{1}$$

$$K = 1.2 \times 10^{16} \times [I]_0^{\alpha} \times \exp(-E_a/RT) \tag{2}$$

where, α, the partial order related to the initiator, is 3.25; E_a, the activation energy, is 9.26 kJ/mol. $[M]$ and $[I]_0$ are monomer and initiator concentration, respectively. R is the universal gas constant. T is the reaction temperature, and t the reaction time. The progression of polymerization is usually characterized with the conversion, C, which is defined as

$$C = \frac{[M]_0 - [M]}{[M]_0} \tag{3}$$

where $[M]_0$ is the initial monomer concentration.

After introducing the conversion, the polymerization can be described by

$$\frac{dC}{dt} = K(1 - C) \tag{4}$$

2.2. Simulation method

FLUENT is a CFD package based on Finite Volume Method. The flow of polymer melt in co-rotating twin screw extruders has been simulated with FLUENT by Wünsch et al. [9] and Ma et al. [10]. Especially in Ma's study, the flow patterns in kneading blocks of an intermeshing co-rotating twin screw extruder, predicted with FLUENT, agree well with the experimental data from Particle Image Velocimetry. This indicates that it is reasonable to employ quasi-steady state analysis method, with FLUENT, in the simulation of processes involving twin-screw extruders. The governing equations for the simulation of reactive extrusion are as follows:

Mass conservation (or continuity) equation

$$\nabla \cdot V = 0 \tag{5}$$

Momentum conservation equation

$$-\nabla P + \nabla \cdot \tau = 0 \tag{6a}$$

$$\tau = \eta[(\nabla V) + (\nabla V)^T] \tag{6b}$$

where the viscosity of the reaction system, η, depending on conversion, temperature and shear rate, can be modeled with the generalized Yasuda–Carreau equation, as discussed by Gimenez et al. [7].

$$\eta(\dot{\gamma}) = \frac{\eta_0}{[1 + (\tau\dot{\gamma})^a]^{(1-n)/a}} \tag{7}$$

where $n = 0.52$, and $a = 1.05$. τ characterizes the shear-stress level at which η is in the transition between Newtonian and shear thinning behavior, given by

$$\tau = 1.7 \times 10^{-20} \times M_w^{4.1} \times \exp\left[\frac{E_b}{R}\left(\frac{1}{T} - \frac{1}{T_0}\right)\right] \tag{8}$$

where E_b is the flow activation energy (40.0 kJ/mol), T_0 is the reference temperature (413 K). $\overline{M}_w$ is the weight averaged molecular weight. The zero-shear viscosity η_0 of poly-ε-caprolactone samples takes two forms:

In the power law zone ($M_w \geqslant M_c$):

$$\eta_0 = 1.35 \times 10^{-17} \times M_w^{4.4} \times \exp\left[\frac{E_b}{R}\left(\frac{1}{T} - \frac{1}{T_0}\right)\right] \times C^4 \times a_\phi \tag{9a}$$

In the Rouse regime ($M_w < M_c$):

$$\eta_0 = 2.24 \times 10^{-5} \times M_w^{1.2} \times \exp\left[\frac{E_b}{R}\left(\frac{1}{T} - \frac{1}{T_0}\right)\right] \times C \times a_\phi \tag{9b}$$

where a_φ represents the free volume correction during polymerization of ε-caprolactone. It can be described by

$$a_\varphi = \exp\left(-\frac{1}{RT}(E_b - E_s)\right) \tag{10}$$

where E_b and E_s are the flow activation energy for the bulk and solution systems, respectively.

Energy conservation equation gives,

$$\rho C_P V \cdot \nabla T = k\nabla^2 T + \tau : \nabla V + Q_R \tag{11}$$

in which k is the thermal conductivity, and Q_R is the rate of reaction heat generation:

$$Q_R = \rho \Delta H \frac{dC}{dt} \tag{12}$$

where ΔH is the reaction heat in polymerization, which for ε-caprolactone, is about 250 kJ/kg [7]. ρ is the density of the reaction system.

In the simulation with FLUENT, the energy source term of heat from reaction (Q_R in Eqs. (11) and (12)) and viscosity of the reaction system (η in Eqs. (6b) and (7)), which depend on the progression of reaction, were calculated with User Defined Functions (UDFs). A UDF is a function programmed by the user that can be dynamically linked with the FLUENT solver to enhance the standard features of the code.

The kinetics equation was incorporated into FLUENT with a User Defined Scalar (UDS). In order to incorporate the kinetics equation into FLUENT, Eq. (4) was reformulated into

$$U\frac{\partial C}{\partial x} + V\frac{\partial C}{\partial y} + W\frac{\partial C}{\partial z} = K(1 - C) \tag{13}$$

where U, V, and W stand for the x-, y-, and z-components of velocity in a three-dimensional Cartesian system. Similarly, the term on the right side of Eq. (13) was calculated with a UDF in FLUENT.

2.3. Simulation domain

In this study, the polymerization of ε-caprolactone in fully-filled conveying elements of a co-rotating fully intermeshing twin-screw extruder was investigated. The geometry specifications of the conveying elements are listed in Table 1. These conveying elements are right-handed, having an axial length of 120 mm. A pair of 20 mm long kneading discs, having identical axial cross section as the conveying element, was attached at the end of the conveying element, to ensure good convergences in the simulation [11]. As will be presented in the next section, the flow is assumed to be fully developed at the exit. However, the flow can hardly reach the fully developed condition near the exit of the screw element, due to the complex nature of the geometry. It is known that the geometry of a kneading disk is simpler than that of conveying element, and the flow at the

Table 1
Dimension of conveying screw elements

Barrel diameter	34 mm
Screw tip diameter	33.4 mm
Centerline distance	30 mm
Screw root diameter	26 mm
Screw tip number	2
Screw pitch	20, 40 or 60 mm

outlet of a pair of kneading paddle is close to be fully developed. Furthermore, in practical application, the conveying element is usually followed by kneading blocks or reversed elements. That is, while the addition of a pair of kneading discs at the outlet of screw element would not affect the flow in the latter, it would simplify the simulation enormously.

The geometry of screw elements used in the simulation is shown in Fig. 1. The mesh of the simulation domain was generated with 8-node, brick elements. The number of elements for the conveying screw element was 179,200, and it was 22,400 for the extensional disc domain. In the discussion which follows, the conveying elements with a pitch of 20, 40 and 60 mm are denoted as SE20F, SE40F, and SE60F, respectively.

It is known that the screw rotates continuously during extrusion processing. Consequently, the geometry of the simulation domain changes in a complete rotational cycle, due to the screw rotation. In the present study, the dynamic motion of the screw in the extruder was treated as a quasi-steady state case, a method currently used in the simulation of extrusion processes, by several researchers [12–16]. A series of meshes are generated for the screw element at different rotation angles. The reaction in these screw channels with different angles was simulated with FLUENT, without tracking the movement of material between successive screw rotations. It was found that the effect of screw rotation angles on reaction progression is not a significant factor in the results. The results presented in the current paper were based on the mesh with an initial angle of zero.

2.4. Boundary conditions

In the simulation, the flow was assumed to be fully developed at the outlet. It was also assumed that the screw surface has an adiabatic condition, and the barrel surface remains at a constant temperature. This was proposed, based on the realistic conditions that exist in extrusion. Usually, during polymer processing, the barrel temperature is pre-set to a certain value, and the heating/cooling system on the barrel is designed to maintain the pre-set temperature. Because the screw diameter is small, and there is no heating/cooling system, the heat transfer at the screw surface is close to adiabatic condition during the processing.

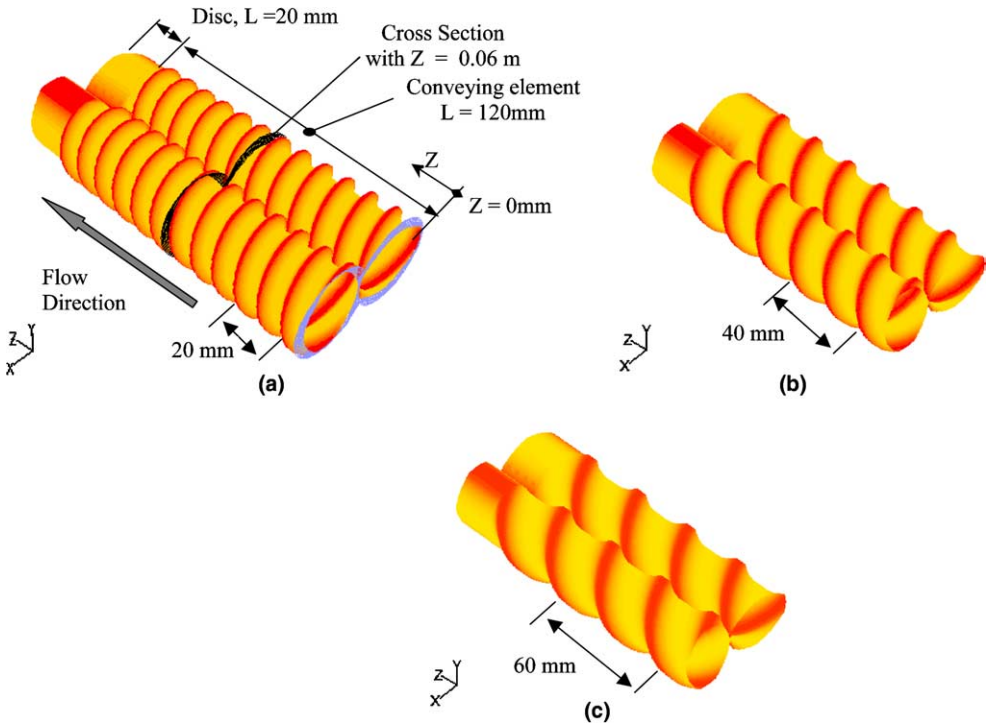

Fig. 1. Geometry of conveying elements: (a) SE20, (b) SE40, (c) SE60.

The axial velocity profile at the inlet was calculated as follows: First, a simulation of Newtonian and isothermal flow in the screw element was carried out, in which the fluid viscosity was calculated based on the temperature and conversion at the inlet, and the axial velocity at the inlet was assumed to have a uniform distribution (calculated according to the flow rate). Next the velocity distribution in the screw channel was obtained, based on the numerical simulation results. Because the screw tip number of the element is 2, the cross section at half of the pitch has the same geometry as the inlet. Hence, the calculated axial velocity profile at an axial location of a half pitch based on Newtonian and isothermal conditions was used as the axial velocity boundary condition at the inlet in the simulation of reactive extrusion.

As shown in Table 2, the ratio of monomer to initiator concentration, $[M]/[I]_0$, was set to 800. The flow rate was 3.15 kg/h; the temperature at channel inlet and barrel surface was 420 K. The screw rotational speed was 48 rpm or 287 rpm. The conversion, which determines the viscosity of the system, was assumed to be 0 or 0.6, at the channel inlet. An inlet conversion of 0.6 was selected here, in order to investigate the effect of viscous dissipation on polymerization, because the system has sufficiently high viscosity when the conversion is higher than this critical value. It was also assumed that the density, thermal conductivity, and heat capacity of the reaction system remained constant during polymerization.

3. Simulation results

Using FLUENT for the simulation of reactive extrusion, several parameters, such as conversion, velocity, temperature, pressure, shear rate and viscosity, were obtained. In this section, the simulation results are presented in two parts, based on the conversion at the inlet.

3.1. Polymerization with a zero inlet conversion

Fig. 2 summarizes the conversion profiles at the top surfaces of the conveying elements SE20F and SE60F, in which the reaction system was conveyed from left to right. The numbers in the plots in Fig. 2 represent the values of conversion. These images show that the patterns of the conversion at screw surfaces depend on screw geometries: with increasing screw pitch, the conversion shows a faster increase for the same screw length.

Fig. 3 shows the conversion distribution at the axial cross section with $Z = 0.06$ m in SE20F and SE60F (see also Fig. 1a), respectively. The numbers in this figure stand for the conversions at the iso-curves. It is seen that the conversion at the axial cross section is not uniform. The distribution of conversion depends on the value of the screw pitch. In SE20F (Fig. 3a), the region with high conversion is located near the barrel surface, whereas in SE60F (Fig. 3b), the maximum conversion appears in the area close to the center of the screw

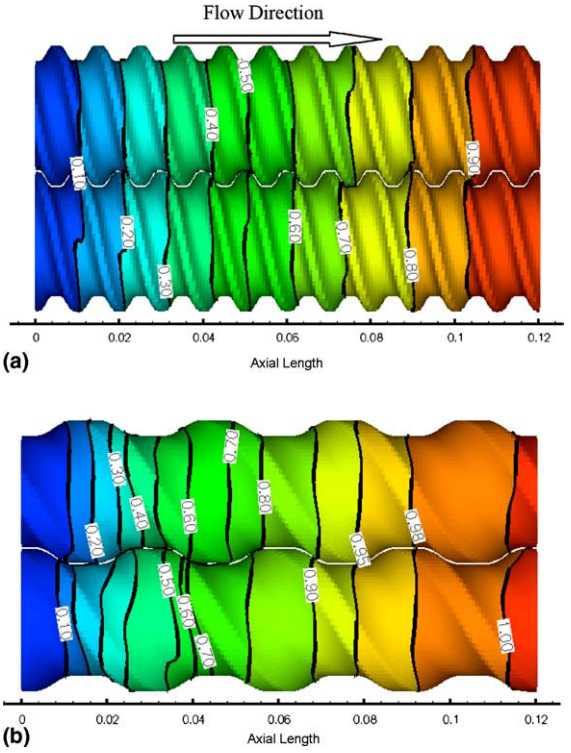

Fig. 2. Conversion profiles at the top surfaces of screw elements for a zero inlet conversion, and a screw speed of 287 rpm: (a) SE20F and (b) SE60F. The numbers in the plots represent the values of conversion.

Table 2
Boundary conditions for simulation

Ratio	Flow rate (kg/h)	Screw speed (rpm)	Barrel temperature (K)	Inlet temperature (K)	Inlet conversion
800	3.15	287	420	420	0
800	3.15	48	420	420	0
800	3.15	287	420	420	0.6
800	3.15	48	420	420	0.6

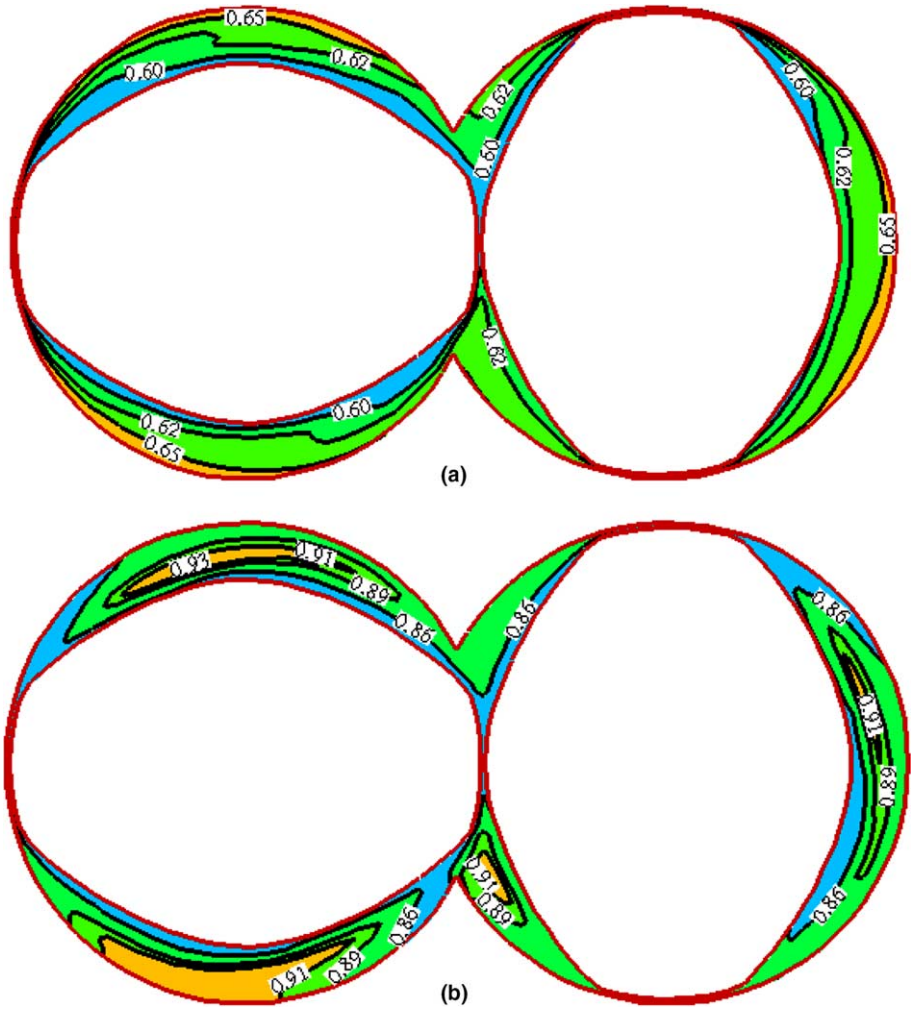

Fig. 3. Conversion profile at axial cross sections of $Z = 0.06$ m in screw elements at a zero inlet conversion and screw speed of 287 rpm: (a) SE20F and (b) SE60F. The numbers in the plots represent the values of conversion at the iso-curves.

channel. However, in both SE20F and SE60F, the conversion near the screw surfaces is lower than that in the remaining regions. Fig. 3 also shows that the values of conversion in SE60F are higher than those in SE20F.

In order to evaluate the profiles of conversion at the axial cross section, the area weighted distribution of conversion was defined, as follows:

$$d(i) = \frac{A(i)}{A} = \frac{A(i)}{\sum_{i=1}^{N_e} A(i)} \tag{14}$$

in which $d(i)$ is the distribution; $A(i)$ is the area with conversion $C(i)$ at an axial cross section; A is the area of the axial cross section; i represents face number in the cross section. Fig. 4 displays the area weighted distributions of conversion at axial cross sections with $Z = 0.01$, 0.04 and 0.07 m in SE20F, and SE60F. The plots in Fig. 4 show that at the cross section with identical axial location, the distribution of conversion becomes broader, and the distribution curves shift to right (high conversion), with increasing screw pitch from 20 to 60 mm.

In order to elucidate the effect of screw pitch on polymerization, the velocity profiles of polymer melt in different conveying elements were investigated. Fig. 5 shows the patterns of the positive axial velocity (i.e., velocity along the downstream direction) in the cross section with $Z = 0.06$ m in SE20F, and SE60F, respectively. In order to increase the clarity of contours, the patterns of the negative axial velocities are not displayed. That is, the blank region in the cross section is the area with negative velocity. Fig. 5 reveals that in the cross section, a large fraction of the fluid elements have negative axial velocity. These fluid elements move upstream, not downstream. Furthermore, the regions with negative velocities in Fig. 5 have high conversion,

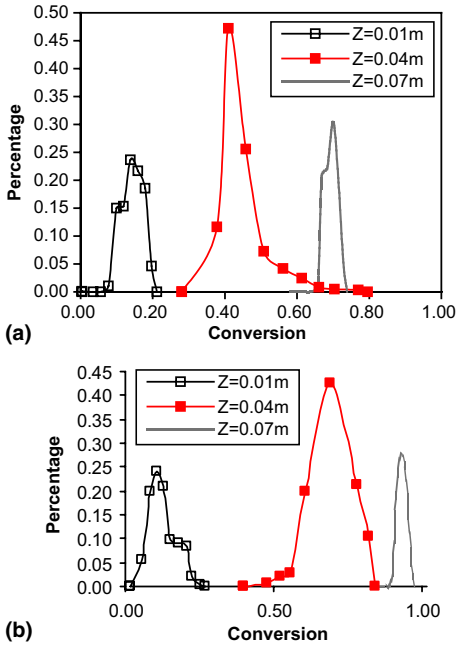

Fig. 4. Conversion distributions at different axial cross sections in screw elements for a zero inlet conversion, and a screw speed of 287 rpm: (a) SE20F and (b) SE60F.

as shown in Fig. 3. On the other hand, the maximum positive axial velocity in SE60F is larger than that in SE20F. This indicates that the axial velocity has a much broader distribution in SE60F than in SE20F. Consequently, SE60F has more intensive mixing potential and broader residence time distribution than SE20F.

The fluid elements in a cross section can be divided into two groups based on the values of axial velocity. That is, the fluid elements with downstream velocities are denoted as forward-flow and those with upstream velocities as back-flow. The forward-flow pushes the reaction system downstream, as the conversion increases along the flow direction. The back-flow carries the fluid upstream. Because the conversion in the downstream is higher than in the upstream, the back-flow helps to increase the conversion at the upstream. Hence, the increase in conversion in the conveying elements is a competing consequence between the forward-flow and back-flow. This implies that the conversion profile depends not only on the ratio of back-flow rate to forward-flow rate, but also on the local distribution of conversion. The latter depends on the temperature profiles in the fluid and residence time distribution. Because the flow rate is identical in both cases, the average residence time in these two elements are the same.

Fig. 6 depicts the calculated results of the area weighted average conversion, temperature, viscosity, pressure and shear rate of the polymerizing system, along the axial length in different conveying elements. Here, the area weighted average parameter at an axial cross section is defined as

$$\bar{\zeta} = \frac{\sum_{i=1}^{N} \zeta(i) A(i)}{\sum_{i=1}^{N_e} A(i)} \tag{15}$$

where $A(i)$ and $\zeta(i)$ are the area and the calculated parameter at cell i, at an axial cross section. N_e is the total number of cells at the cross section.

Fig. 6a shows that, globally, the conversion has a fast increase with increasing screw pitch, from 20 to 60 mm. As discussed previously, this is due to the fact that the mixing is enhanced when the screw pitch is increased. With decreasing screw rotational speed, the reaction becomes faster. This can be attributed to the weak heat transfer at the barrel surface at low screw speed (see Fig. 7).

Fig. 6b reveals that the temperature profile along the axial length depends on the screw rotational speed. When the screw speed was 287 rpm, the temperature rose monotonously along the axial length. At 48 rpm, the temperature increased first, reaching a maximum value at a certain location close to the channel entrance, before dropping gradually. Furthermore, the maximum temperature at 287 rpm was lower than that at 48 rpm. This is due to the fact that the heat from reaction, which depends on the increase in conversion, is the dominant energy source. The heat released from reaction raises the temperature of the system, which, in turn, accelerates the reaction. As shown in Fig. 6a, at 48 rpm, the conversion has a fast increase, jumping to near one in a very short axial distance along the channel, and causing the appearance of the temperature peak there. The low increase in temperature at 287 rpm near the channel inlet was due not only to the small increase in conversion, but also to the large heat loss at the barrel surface.

The decrease in temperature beyond $Z = 0.03$ m at 48 rpm (Fig. 6b) indicates that the heat transfer between the reaction system and barrel surfaces plays an important role there. Because the temperature at barrel surfaces remains constant during polymerization and the screw surface was assumed to have an adiabatic condition, the reaction system with high temperature would release its energy through the barrel surface. Considering the fact that the reaction is complete at an axial location of about 0.03 m, the downstream temperature beyond this location depends on the competition between viscous dissipation and heat loss at the barrel surface. Although the viscosity of the system is quite high at 48 rpm (reaching 800 Pa s at the channel exit, as shown in Fig. 6c), the average shear rate is very low (about 40 s^{-1}, in Fig. 6e). Meanwhile, the melt temperature was much higher than the barrel temperature, which was set at 420 K. This implies that the heat loss at the barrel surface was larger than the viscous dissipation, leading to the decrease in temperature along the axial

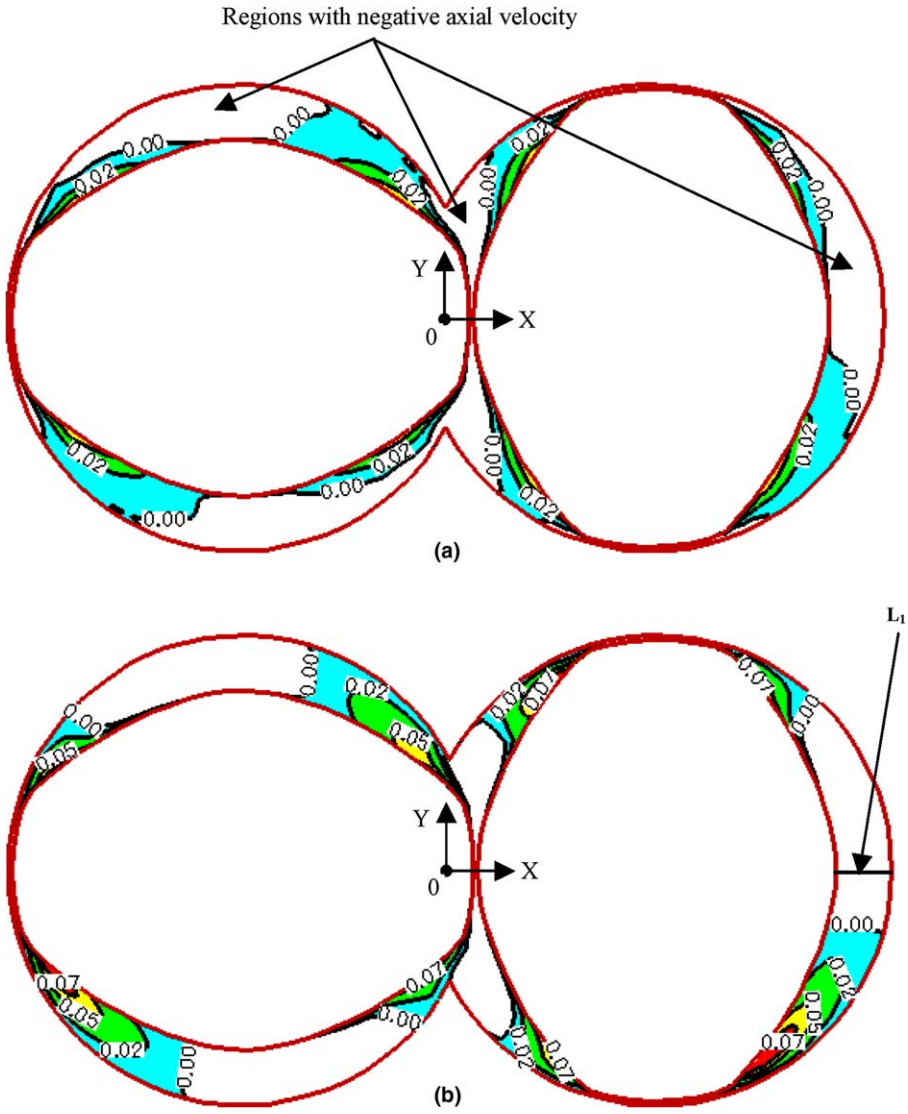

Fig. 5. Axial velocity profiles at axial cross section of $Z = 0.06$ m for $[M]/[I]_0 = 800$ and $N = 287$ rpm in screw elements: (a) SE20F and (b) SE60F [SE60F has a pitch of 60 mm, and the pitch of SE20F is 20 mm. The flow rate in these two cases is identical].

length beyond $Z = 0.03$ m, at 48 rpm. The monotonous increase in temperature along the channel at 287 rpm is attributable to the fact that at this screw rotational speed, the conversion increases gradually along the axial length, and the polymerization is not completed until the mixture has reached the location close to a channel exit.

In the simulation, the inlet pressure was set to zero. Thus, a positive pressure at the channel exit means that the screw element builds up pressure, while a negative pressure means that the pressure is consumed in an element, i.e., the inlet has a higher pressure than the outlet. Fig. 6d shows the average pressure in the cross section along the axial length. It is seen that the average pressure rises along the axial length. For SE40F and SE60F, the average pressure at the channel exit increases with increasing screw speed. However, the average pressure at the exit of SE20F is lower at 287 rpm than that at 48 rpm. This can be explained by the fact that the pressure gradient in conveying elements depends not only on the screw speed, but also on the system viscosity and screw geometry. It is known that when the leaking flow is neglected, the relationship between net flow rate, Q, drag flow, Q_D, and pressure flow, Q_P, in conveying elements can be given by [17]

$$Q = Q_D - Q_P \tag{16}$$

in which drag flow rate and pressure flow rate can be represented by

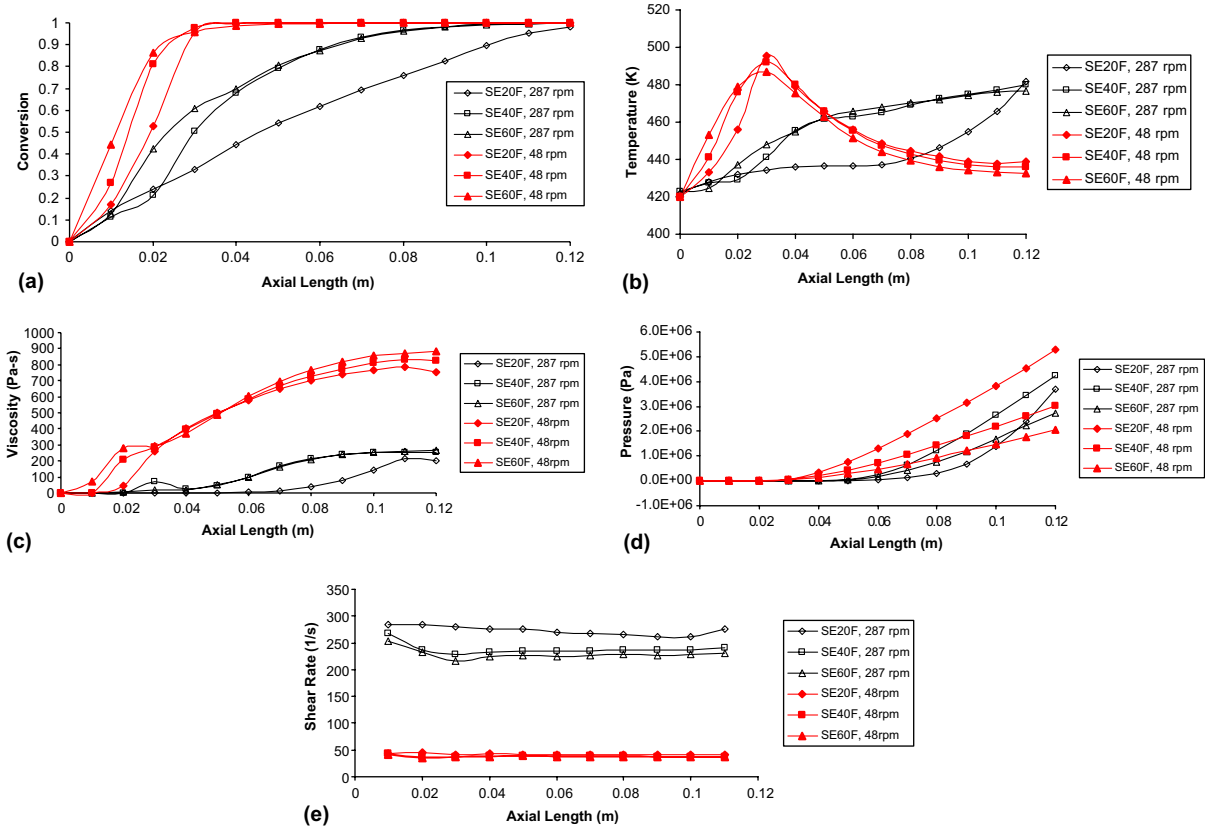

Fig. 6. Area weighted average parameters along the axial length of screw elements during polymerization for a zero inlet conversion: (a) conversion, (b) temperature, (c) viscosity, (d) pressure, and (e) shear rate.

$$Q_{\mathrm{D}} = \chi N \tag{17a}$$

$$Q_{\mathrm{P}} = \lambda \frac{P}{\mu} \tag{17b}$$

where χ and λ are constants depending on the screw geometry. N is the screw rotating speed, P the pressure increase in the element. μ is the system viscosity. Eqs. (16) and (17) can be reformulated into

$$P = \frac{\mu}{\lambda}(\chi N - Q) \tag{18}$$

Eq. (18) indicates that the pressure drop decreases with decreasing viscosity, but increases with increasing screw rotating speed. As shown in Fig. 6c, the system viscosity in SE20F is very small at 287 rpm, which is much lower than that at 48 rpm. Consequently, the pressure at exit of SE20F is low at 287 rpm. Fig. 6e shows that the effect of screw geometry on average shear rate is negligible at 48 rpm, but is quite significant at 287 rpm.

In order to explain the effect of screw rotational speed on the heat transfer at the walls, the velocity profile along line L_1 in SE60F (see Fig. 5b; this is a line from the screw surface to barrel inner surface at $Y = 0$ m in the cross section with $Z = 0.06$ m) was determined and displayed in Fig. 7. It is seen that with decreasing screw speed, the velocity gradient near the barrel surface drops. It is known that the heat loss through the barrel surface depends on the convection near the wall, which, in turn, depends on the velocity gradient. The small gradient in velocity implies low convection near the wall, leading to the decrease in the heat loss through the barrel. Consequently, more heat from reaction is retained in the reaction system at a low screw speed, resulting in a faster polymerization. This suggests that the polymerization of ε-caprolactone in screw channels is a complex process, which depends not only on the flow and mixing characteristics of the reaction system, but also on the heat generation and heat transfer in the extruder.

3.2. Polymerization with an inlet conversion of 0.6

Here, the conversion at the inlet of conveying elements was assumed to be 0.6, whereas it was set to 0 in the preceding studies. Because the viscosity of the system is correlated to the conversion, it is expected that the system viscosity near the inlet would be higher than that

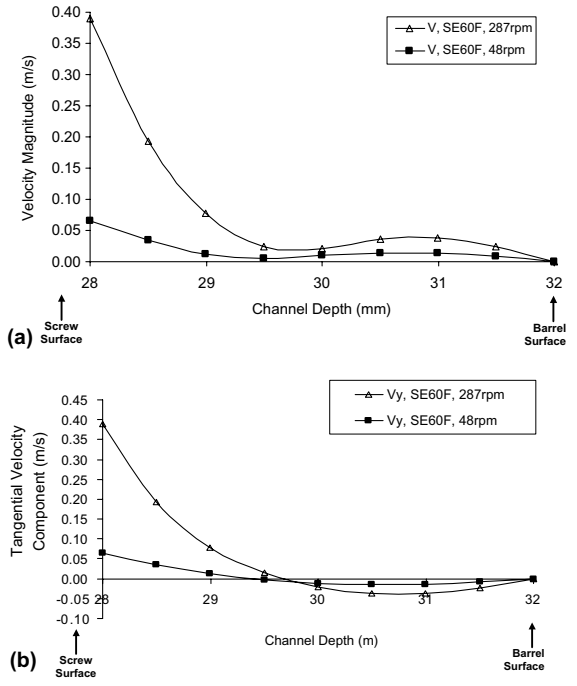

Fig. 7. (a) Velocity magnitude and (b) tangential velocity component (at Y direction) along line L_1 in SE60F (see Fig. 5b).

in the previous cases. Thus, the viscous dissipation could play an important role in the polymerization. On the other hand, the maximum increase in conversion in the screw elements depends on the inlet conversion. It is known that the conversion is 1.0, when the polymerization has completed (see Eq. (3)). At an inlet conversion of 0.6, the maximum increase in conversion would be 0.4 (increase from 0.6 to 1.0), whereas it is 1.0 when the inlet conversion is 0 (increase from 0 to 1.0). Accordingly, the heat from reaction would be smaller at an inlet conversion of 0.6.

Fig. 8 shows the simulation results for the polymerization progression with a conversion of 0.6 at the channel inlet. Unlike the results in Fig. 6a, the trend in Fig. 8 is that of a gradual increase in conversion with axial length. Fig. 8 reveals that the conversion at 48 rpm is lower than that at 287 rpm. This trend is different from those presented in Fig. 6a. The plausible reasons for this trend are presented in the following paragraphs.

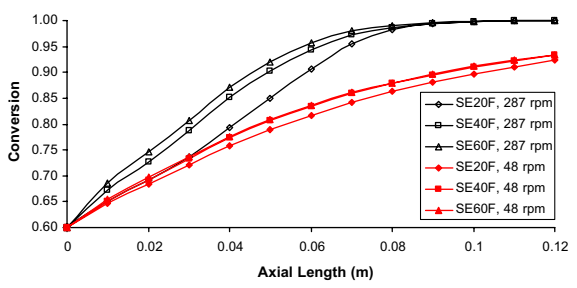

Fig. 8. Area weighted average conversion along the axial length during polymerization at an inlet conversion of 0.6.

The reduction in screw rotational speed would give rise to three possible outcomes: (1) The axial mixing and transverse mixing in the conveying elements would decrease at low screw speed, which would slow down the reaction progression. (2) The convection in the reaction system near the barrel surface drops with decreasing screw speed, leading to a decrease in heat loss through the barrel surface, which, in turn, would result in an increase in temperature (see Fig. 6b) and an acceleration in the reaction. (3) The shear rate decreases when the screw rotational speed drops (see Fig. 6e), resulting in a decrease in viscous dissipation heat. As a consequence, the temperature might fall, and the reaction could slow down.

In order to elucidate the interrelationships among heat from reaction, viscous dissipation, and heat transfer at the walls in the extrusion polymerization, three cases with different thermal conditions have been studied: (1) An adiabatic reaction, i.e., the system has no energy loss during reaction. (2) A constant temperature at barrel surface, but neglecting viscous dissipation of the reaction system, i.e., the viscous dissipation term is not included in the energy equation (see Eq. (11)). (3) A constant temperature at barrel surface, and considering viscous dissipation of the reaction system, as investigated in the current study (see Table 2).

Fig. 9 shows the increases in average conversion along the axial length of SE20F with various thermal conditions during reaction. The results in Fig. 9 show that the reaction is the fastest under the assumption of adiabatic conditions, and slowest in the cases when the viscous dissipation was excluded. At the adiabatic condition, the reaction was faster at 287 rpm than that at 48 rpm. This confirms the hypothesis that the increases in back-mixing and viscous dissipation at high screw

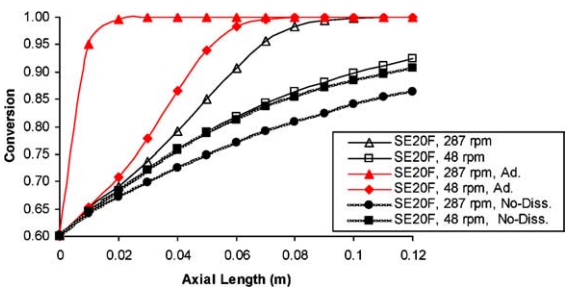

Fig. 9. Effects of heat transfer conditions at the wall on average conversions for an inlet conversion of 0.6 (Ad. represents adiabatic condition, No-Diss. stands for the case in which the viscous dissipation is neglected).

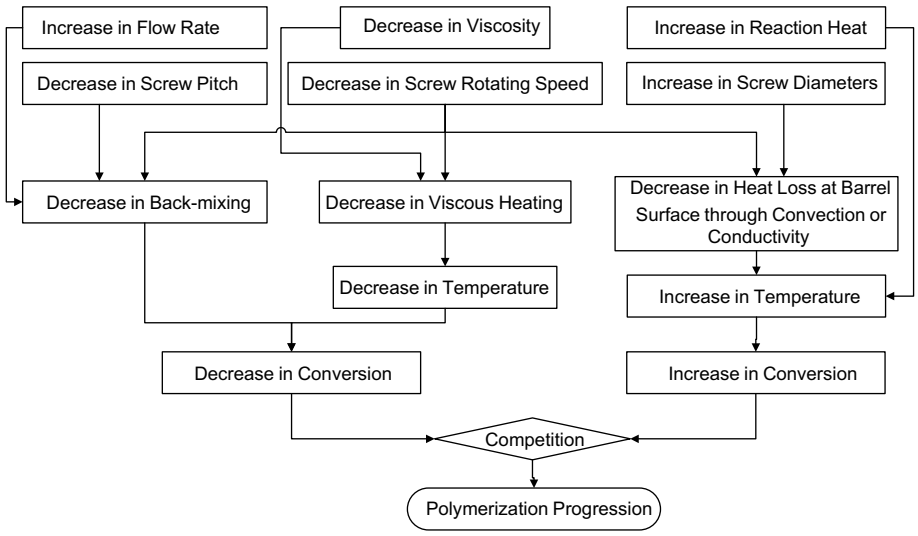

Fig. 10. A flow diagram illustrating the factors affecting polymerization in conveying elements.

speed favor the polymerization progression. In the case without viscous dissipation, the polymerization at 287 rpm is slower than that at 48 rpm. This can be explained by the fact that the heat loss at barrel surface is small at low screw rotational speed. Accordingly, in the case when the viscous dissipation was included and the barrel surface was assumed to maintain constant temperature during polymerization, which was the situation investigated in the present study (Table 2), the reaction progression depends on the competition between the heat loss at barrel, viscous dissipation and heat from reaction. In this case, the viscous dissipation plays an important role in the polymerization process, because the conversion at the channel inlet is 0.6. With decreasing screw speed, both the viscous dissipation and mixing intensity drop, leading to the decrease in temperature and conversion. This result would explain why the increase of conversion along the axial length of the conveying elements drops with decreasing screw speed, as shown in Fig. 8. In the cases presented in Fig. 6, the key energy source is not viscous dissipation, but the heat from reaction and the heat loss through the wall; the latter decreases at low speed.

4. Conclusions

In this study, the effects of screw geometries, screw rotational speed, and initial conversion at channel inlet on polymerization kinetics were analyzed with a commercial CFD package. The results show that the polymerization kinetics in the conveying elements is very complex. The extent of polymerization is the result of competition among such factors as mixing intensity, heat transfer at the barrel surface, viscous dissipation, and heat from reaction.

The dependence of polymerization of ε-caprolactone in the conveying elements on screw geometry and operational conditions can be interpreted in terms of the energy balance during the reaction, as illustrated in Fig. 10. When the reaction system has a low viscosity (say, when the inlet conversion is 0), the viscous dissipation is not a key factor in the energy balance, whereas the heat from reaction can be a dominant factor. With decreasing screw speed, the heat loss at barrel surface drops, and thus the reaction accelerates. On the other hand, when the system has a high viscosity (say, when the inlet conversion is 0.6), the viscous dissipation plays an important role in the energy generation, which drops at low screw speed. Accordingly, the reaction slows down at low screw speed.

References

[1] S.B. Brown, Reactive extrusion, a survey of chemical reactions of monomers and polymers during extrusion processing, in: M. Xanthos (Ed.), Reactive Extrusion, Principles and Practice, Hanser Publishers, Munich, 1992 (Chapter 4).
[2] G.-H. Hu, M. Lambla, Fundamentals of reactive extrusion: an overview, in: R.W. Cahn, P. Hassen, E.J. Kramer (Eds.), Encyclopedia of Materials: Science and Technology, vol. 18, Elsevier Science, Oxford, 1997 (Chapter 6).
[3] C. Tzoganakis, Reactive extrusion of polymers: a review, Adv. Polymer Technol. 9 (1989) 321–330.
[4] G.H. Hu, Reactive blending in screw extruders, in: W. Baker, C. Scott, G.-H. Hu (Eds.), Reactive Polymer Blending, Hanser Publishers, Munich, 2001 (Chapter 6).

[5] J.L. White, Simulation of flow in intermeshing twin-screw extruders, in: I. Manas-Zloczower, Z. Tadmor (Eds.), Mixing and Compounding of Polymers: Theory and Practices, Hanser Publishers, Munich, 1994 (Chapter 10).
[6] D.B. Todd, Features of extruder reactors, in: M. Xanthos (Ed.), Reactive Extrusion, Principles and Practice, Hanser Publishers, Munich, 1992 (Chapter 5).
[7] J. Gimenez, Ph. Cassagnau, R. Michel, Bulk polymerization of caprolactone: rheological predictive law, J. Rheol. 44 (2000) 527–547.
[8] A. Poulesquen, B. Vergnes, Ph. Cassagnau, J. Gimenez, A. Michel, Polymerization of ε-caprolactone in a twin screw extruder, experimental study and modeling, Int. Polymer Process. 16 (2001) 31–38.
[9] O. Wünsch, R. Kühn, P. Heidemeyer, Simulation of the fluid flow of deeper screw flights for co-rotating twin screw extruders, Proceedings of 61st SPE ANTEC, vol. 1, Society Plastics Engineers, 2003, pp. 338–343.
[10] R. Ma, A.N. Hrymak, P.E. Wood, Numerical simulation and experimental verification of flow field in a twin screw extruder, in: Proceedings of 17th Annual Meeting of Polymer Processing Society (CD-ROM), Society of Polymer Processing, 2001.
[11] Th. Avalosse, Y. Rubin, L. Fondin, Non-isothermal modeling of co-rotating and contra-rotating twin screw extruders, Proceedings of 58th SPE ANTEC, vol. 1, Society Plastics Engineers, 2000, pp. 19–24.
[12] T. Fukuoka, Numerical simulation of a reactive extrusion processing. Part II. Simulation and verification for the twin screw extrusion, Polymer Eng. Sci. 40 (2000) 2524–2538.
[13] D. Strutt, C. Tzoganakis, T.A. Duever, Mixing analysis of reactive polymer flow in conveying elements of a co-rotating twin screw extruder, Adv. Polymer Technol. 19 (2000) 22–33.
[14] H. Yang, I. Manas-Zloczower, Flow field analysis of the kneading disc region in a corotating twin screw extruder, Polymer Eng. Sci. 32 (1992) 1411–1417.
[15] V.L. Bravo, A.N. Hrymak, J.D. Wright, Numerical simulation of pressure and velocity profiles in kneading elements of a co-rotating twin screw extruder, Polymer Eng. Sci. 40 (2000) 525–541.
[16] L. Zhu, K.A. Narh, K.S. Hyun, 3-D Modeling of polymerization in conveying element in twin-screw extruder, Proceedings of 61st SPE ANTEC, vol. 1, Society Plastics Engineers, 2003, pp. 147–151.
[17] M.L. Booy, Isothermal flow of viscous liquid in corotating twin-screw device, Polymer Eng. Sci. 20 (1980) 1220–1227.